Novel Electrochemical Approach to Discriminate the Coordination of Two Polymers Using Polymer-Modified Carbon Paste Electrodes

S. Loughmari[1*], M. Oubaouz[2], M. Oukbab[2], H. Haddouchy[3], M.Visseaux[4], A. El Bouadili[1], S.-E. El Qouatli[3] and A. Chtaini[2]

[1] *Laboratory of Industrial and Surface Engineering, Applied Chemistry and Environmental Sciences Team, Faculty of Sciences and Technology, Sultan Moulay Slimane University, Beni-Mellal, Morocco*
[2] *Molecular Electrochemistry and Inorganic Material Team, Faculty of Sciences and Technology, Sultan Moulay Slimane University*
[3] *Physical Chemistry Environment and Materials, Faculty of Sciences and Technology, Moulay Ismail University, Boutalamine, Errachidia, Morocco*
[4] *University of Lille, CNRS, Central Lille, University Artois, UCCS, Catalysis and Slide Chemistry Unit, Lille, France*
*Corresponding author: salihaloughmari@gmail.com

Received 15/09/2024; accepted 20/02/2025
https://doi.org/10.4152/pea.2027450102

Abstract

To discriminate the structures of two polymers, 1,4-transpolymyrcene (TPM) and 1,4-cis polymyrcene (CPM), at molecular level, nuclear magnetic resonance (NMR) was herein used as the main method. However, to enhance the reliability of findings, this method involves a longer ordering time, which results in higher costs. A simple electrochemical technique, based on the use of cyclic voltammetry (CV), square wave voltammetry (SWV) and electrochemical impedance spectroscopy (EIS), was incorporated into the approach of this study. CV provided information on the polymers' electronic properties, while EIS enabled to assess electrochemical properties and conductivity. These techniques were utilized to identify distinctions between TPM and CPM, without resorting to NMR analysis, and they provided crucial data on the polymers' structure and electrochemical behavior. By comparing results obtained by these two approaches, the validity of conclusions drawn from NMR analysis was confirmed. This hybrid approach, combining advanced NMR techniques with electrochemical methods, enabled a more comprehensive characterization of TPM and CPM. Thus, it offers an integrated and more reliable approach to molecular structure discrimination, enhancing the understanding of natural polymers in diverse applications.

Keywords: CPM; CV; EIS; NMR analysis; SWV; TPM.

Introduction[•]

Electrochemistry offers a fascinating insight into characteristics and behaviors of polymer-based materials. Recently, chemical researchers, particularly in the field

---

[•] The abbreviations list is in page 25.

of electrochemistry, have developed several sensors aimed at distinguishing between organic molecules, such as drugs, including antibiotics like Metronidazole (MNZ) or hydroxychloroquine and nitrofurazone [1-3]. These advancements also have applications in the environmental field, notably for detecting pollutants such as heavy metals in water and food analysis [4].

Despite its medicinal properties, MNZ contributes to the aforementioned problems, since, as a soluble, non-biodegradable compound, it accumulates in aquatic ecosystems [5]. Thus, sensors using glassy carbon electrodes enriched with carbon nanotubes have been developed to detect MNZ [6]. However, this modification requires electropolymerization of carbazole, with a high oxidation potential and a slow polymerization rate. To overcome this limitation, modifications have been implemented in carbazole monomer, for reducing its oxidation potential, thereby enabling the control of optical and electronic properties of this polymer [7].

The consideration of plant-derived products as potential source of raw materials for chemistry is a fundamental criterion of sustainable chemistry. This concern is due to their renewable nature and inherent biodegradability of their structure. The valorization of these compounds into higher value-added products is a constant challenge. Terpenes derived from citrus fruits or resinous sources are among these naturally occurring molecules that hold potential for such valorization. Being derived from biomass, they are generally inexpensive compounds. Terpenes are natural substances abundant in Mediterranean ecosystems, among which Myrcene ($C_{10}H_{16}$) is notable. They are found particularly in essential oil of oregano (*Origanum compactum*, *Lamiaceae* family) and in mastic tree, both of which are highly prevalent plants in High and Middle Atlas regions of Morocco. This monoterpene may be obtained with high yield through simple thermal isomerization of β-pinene derived from turpentine oil [8]. Due to a recent increasing demand for bio-derived polymers, terpene resins are utilized in various pharmaceutical syntheses of vitamins and insecticides [9]. Furthermore, thermoplastic polymers hold significant industrial importance, due to their employ across a wide range of applications, including adhesives, elastomers, composite materials and impact-resistant transparent materials [10].

Several methods have been employed to polymerize this monoterpene. $C_{10}H_{16}$ has been polymerized using reversible transfer methods [11]. PM has also been synthesized using a system based on cobalt complexes [12]. Through coordination, this acyclic monoterpene has been polymerized, copolymerized and terpolymerized by lanthanide catalysts [13-16]. Thermoplastic elastomers based on $C_{10}H_{16}$ have also been obtained through anionic copolymerization [17], cationic emulsion copolymerization [18] and controlled radical copolymerization [19] of this monomer with other ones.

PM offers opportunities as a potential component of sustainable materials for many applications. This bioresource monomer is also used in latex synthesis to create value-added products that can be used in coatings industry for the fabrication of many products, including paints, varnishes, coatings, adhesives, paper coatings, binders in paper and textile products [20, 21].

In this study, the research objective was to fabricate a CPE that could distinguish between 1,4-cis polymyrcene (CPM) and 1,4-transpolymyrcene (TPM), with excellent electrochemical performance. Herein, there was also an interest in the interaction between polymer units and CPE. The polymers electrochemical behavior was examined using CV, a technique that identifies oxidation and reduction reactions of the polymers with the electrode. In addition, EIS and SWV were used to complete the analyses.

Materials and methods

Synthesis section

The experimental procedure was conducted within a dry argon environment, either using a glove box or Schlenk techniques. Toluene underwent purification by passing it through an alumina column (Mbraun SPS), and it was subsequently stored on molecular sieves (3A) in the glove box, after being distilled from sodium/benzophenone ketyl traps. The monomer ($C_{10}H_{16}$) acquired from Aldrich was dried over calcium hydride, then distilled over molecular sieves, and once again prior to utilization. $Nd(BH_4)_3(THF)_3$ was synthesized following established literature procedures [22]. The following chemicals were utilized in their original forms: $B(C_6F_5)_3$ (97%, Strem Chemicals), $Al(i\text{-}Bu)_3$ (Aldrich) and BEM (20 wt% in heptane from Texas Alkyls).

In Size Exclusion Chromatography, Tetrahydrofuran (THF) was employed as eluent, at 40 °C, with a flow rate of 1 mL/min. The system consisted of Waters SIS HPLC pump, Waters 410 refractometer and Waters Styragel column (HR2, HR3, HR4 and HR5E) calibrated using polystyrene standards.

For proton (^1H) and carbon-13 NMR (^{13}C), spectra of the polymers were recorded at 300 K, using Bruker Avance 300 spectrometer in Chloroform-D1 as solvent.

Differential Scanning Calorimetry analyzes were performed in a nitrogen-controlled atmosphere using Setaram 141 apparatus. Samples weighing approxim. 30 mg were placed in aluminum crucibles, and subjected to a heating rate of 10 °C/min, within a range from -120 to 100 °C.

Electrochemical measurements

Electrochemical experiments were conducted using VoltaLab potentiostat (model PGSTAT 100, Eco Chemie BV, Utrecht, The Netherlands), driven by general purpose electrochemical systems data processing software (VoltaLab master 4 software). The measuring cell used in this work was a three-electrode cuvette, with polymer-modified CPE, saturated calomel and platinum plate serving as working, reference and auxiliary electrodes, respectively.

Results and discussion

Synthesis section

CPM

The microstructure of the resulting PM using this ternary catalytic system ($Nd(BH_4)_3(THF)_3/B(C_6F_5)_3/Al(i\text{-}Bu)_3$) [13] was examined using ^{1}H NMR and ^{13}C NMR analyses. ^{1}H NMR spectrum depicted in Fig. 1 exhibit distinct signals representing different hydrogen atoms within PM structure. The signal detected from 5.06 to 5.19 ppm is attributed to olefinic resonances, which correspond to double bonds present in PM.

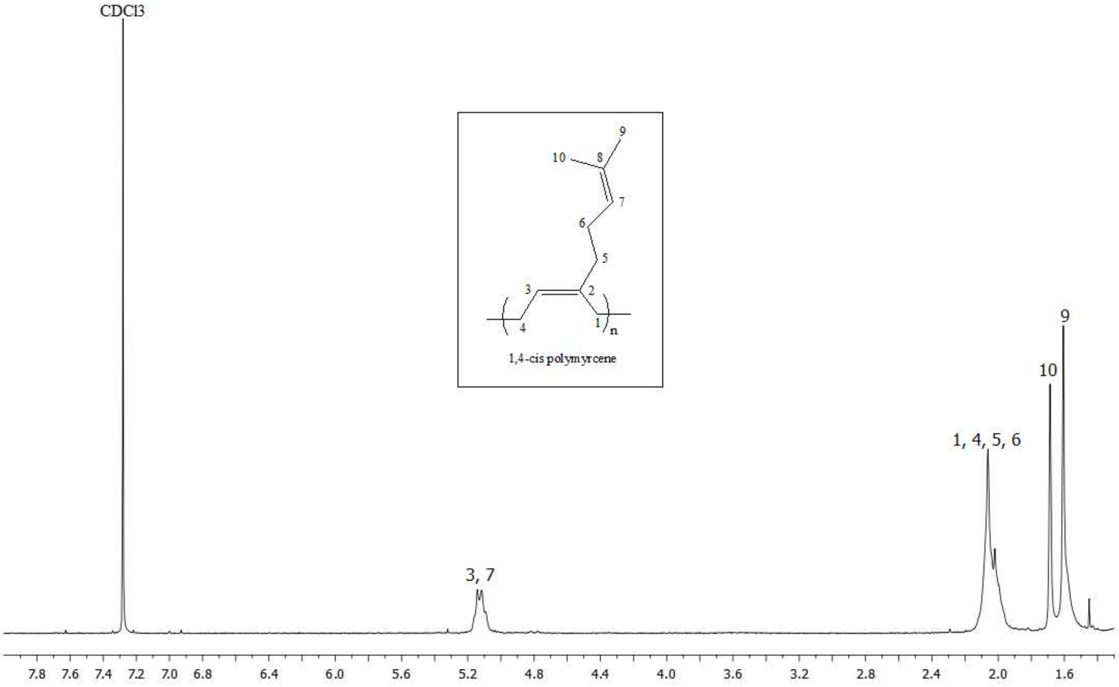

Figure 1: ^{1}H NMR spectrum of CPM.

The signal range from 1.92 to 2.19 ppm corresponds to CH_2 of 1,4-cis unit from PM. Other discernible signals at 1.60 and 1.67 ppm are associated with methyl protons within PM structure.

^{13}C NMR analysis (Fig. 2) is in accordance with the structure of obtained CPM, presenting 10 signals corresponding to $C_{10}H_{16}$ within the polymer.

Signals can be divided into two categories: six aliphatic carbons (designated as 1, 4, 5, 6, 9 and 10) and four olefinic carbons (2, 3, 7 and 8). Olefinic spectrum exhibited two quaternary carbons with highest chemical shifts, C2 and C8, at 139.07 and 131.27 ppm, respectively. Additionally, two CH groups were observed at approxim. 124.60 ppm (C7 and C3). In the aliphatic segment of the spectrum, the two most shielded signals corresponded to CH_3 groups inherent in $C_{10}H_{16}$ (C9 and C10, at 17.78 and 25.77 ppm, respectively). The remaining three signals represent methylene groups (C4, C5, C6 and C1, at 26.88, 27.04, 30.70 and 37.00 ppm, respectively).

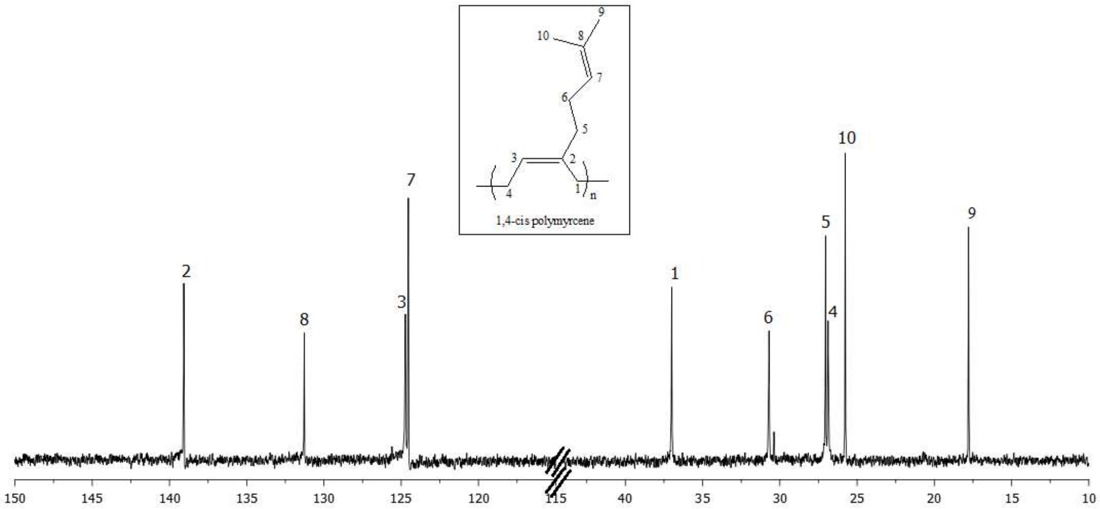

Figure 2: ^{13}C NMR spectrum of CPM.

TPM

PM was synthesized using biosourced $C_{10}H_{16}$ in the presence of $Nd(BH_4)_3(THF)_3$-based coordination catalyst combined with BEM. Successful production of TPM was achieved (Fig. 3) with 84% yield, at 70 °C, for 2 h [13].

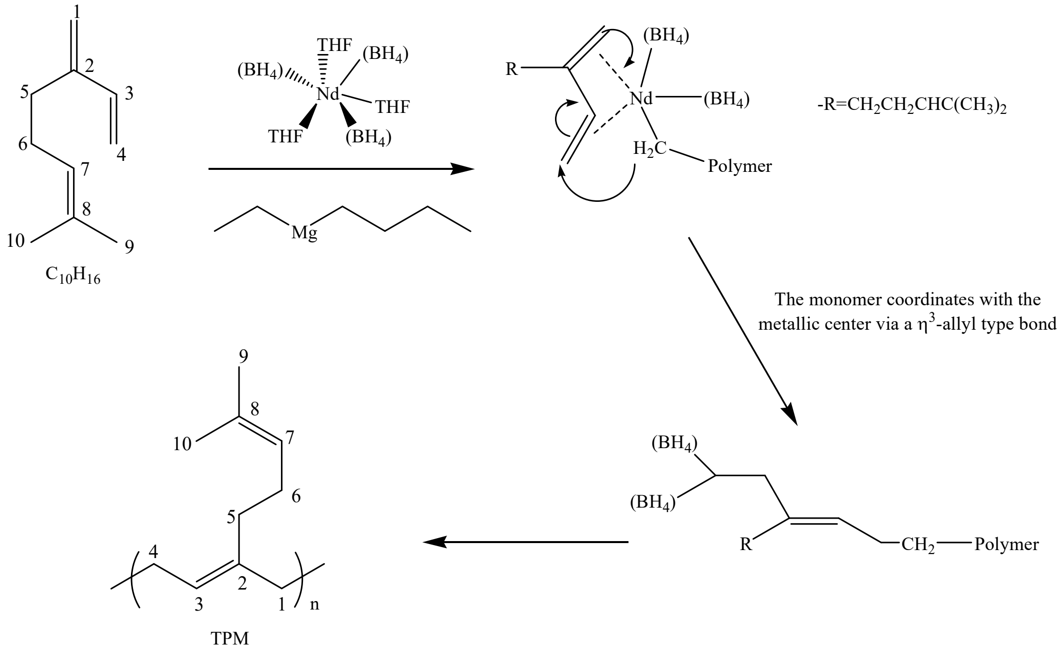

Figure 3: η^4 coordination of $C_{10}H_{16}$, leading to 1,4 insertion.

Analyses were conducted using spectroscopic methods, including ^{1}H-NMR (Fig. 4) and ^{13}C-NMR (Fig. 5). Resulting PM exhibited a predominant microstructure of TPM (up to 90.8 %).

^{1}H-NMR spectrum (Fig. 4) indicates the presence of CH_3 within TPM unit of PM, as evidenced by the signal range from 1.50 to 1.75 ppm. Moreover, the signal observed at 2 ppm is associated with CH_2 protons within PM structure, while the signal at 5.2 ppm is attributed to olefinic protons, corresponding to double bonds present in PM.

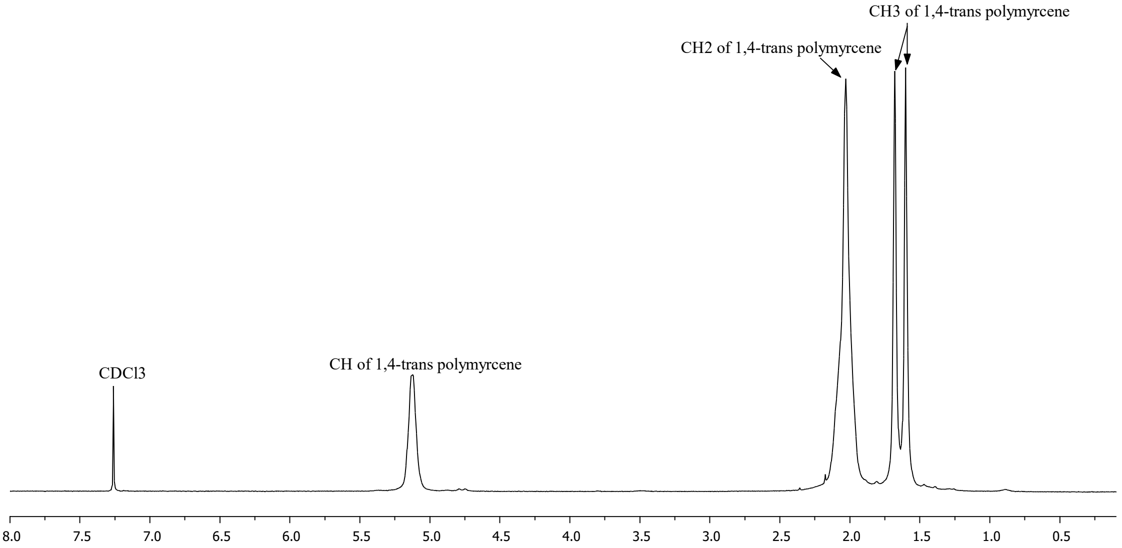

Figure 4: ^{1}H NMR spectrum of TPM.

In accordance with the structure of obtained TPM, ten signals assigned to $C_{10}H_{16}$ within the polymer were seen during ^{13}C-NMR (Fig. 5).

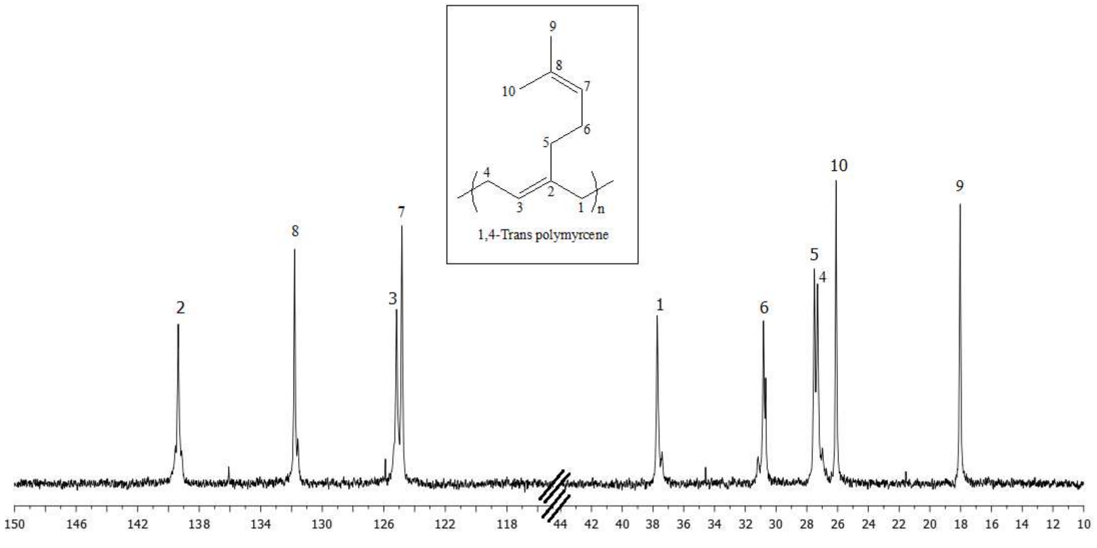

Figure 5: ^{13}C NMR spectrum of TPM.

Six signals arose from aliphatic carbons (designated as 1, 4, 5, 6, 9 and 10), while four signals originated from olefinic carbons (2, 3, 7 and 8). In the region of the spectrum associated with double bonds, two quaternary carbons exhibited highest chemical shifts, C2 and C8, at 139.36 and 131.80 ppm, respectively. Two CH groups were also evident at around 124.80 ppm (C7 and C3). In aliphatic section of the spectrum, the two most shielded signals corresponded to CH_3 groups specific to $C_{10}H_{16}$ (C9 and C10, at 17.82 and 26.10 ppm, respectively), while the remaining three signals represented methylene groups (C4, C5, C6 and C1, at 26.99, 27.30, 30.67 and 37.72 ppm, respectively).

Application by electrochemical methods

Fig. 6 shows CV of CPE and CPE-TPM in a 1 M NaCl electrolyte medium, at a scan rate of 50 mV/s. The increase in anodic current can be attributed to oxidation of the polymer formed on the CPE surface. Conversely, the increase in cathodic current may be associated with the reduction of TPM monomers at the CPE surface. The higher the monomer concentration, the greater the number of monomers available for reduction.

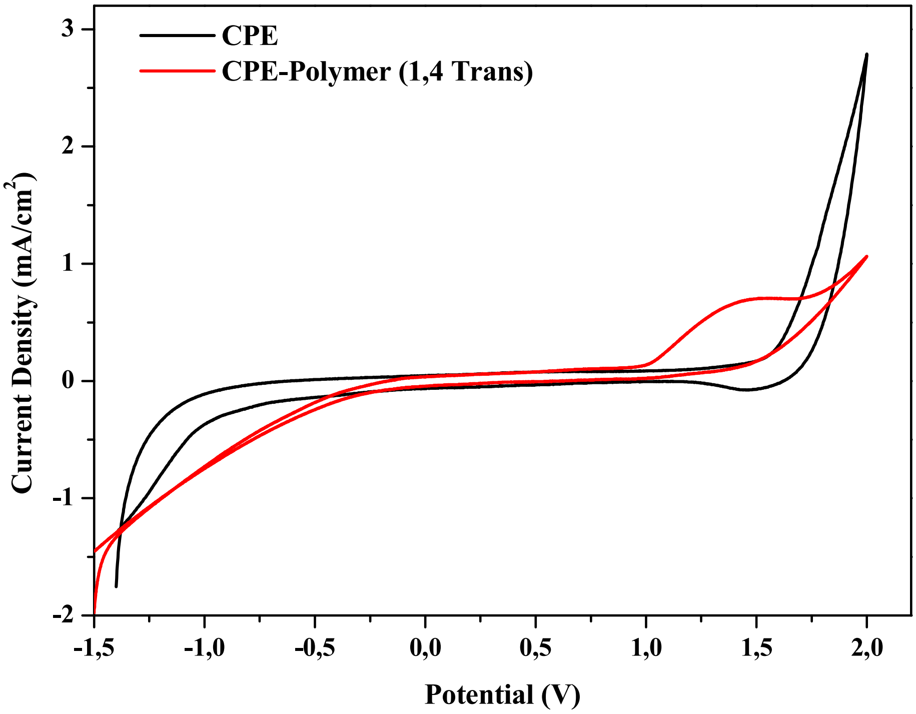

Figure 6: CV of CPE and CPE-TPM in 1 M NaCl at a scan rate of 50 mV/s and PH 7.

Fig. 7 shows CPE and CPE-CPM immersed in a 1 M NaCl electrolyte solution, at a scan rate of 50 mV/s. The polymer covered the electrode surface, reducing the number of sites available for reagents adsorption. One hypothesis suggests that CPM generated pores in CPE matrix, potentially influencing the diffusion of reagents towards the active surface. In conclusion, it is conceivable that CPM possesses variable electrical conductivity compared to CPE, which could influence electrode resistance and electron transfer.

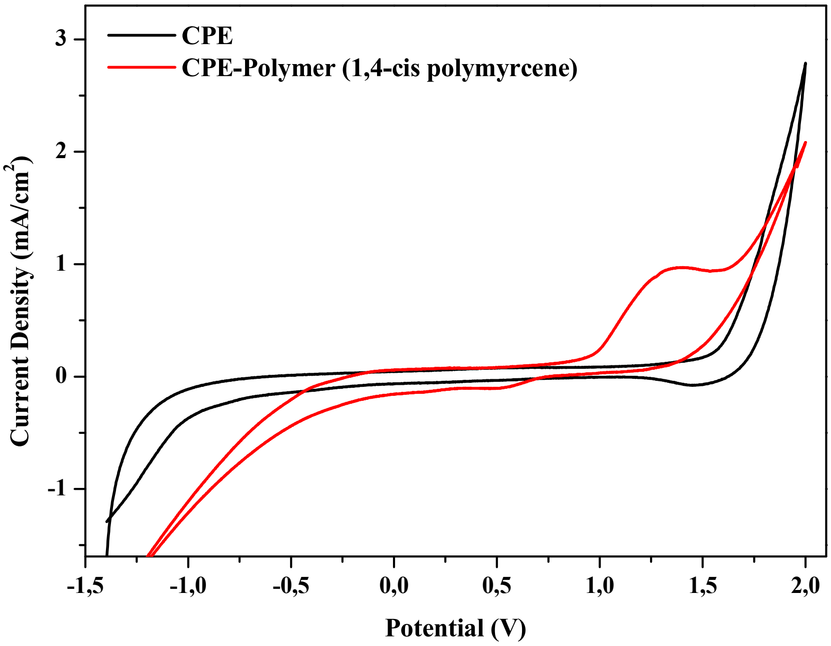

Figure 7: CV of CPE and CPE-CPM in 1 M NaCl at a scan rate of 50 mV/s and PH 7.

Fig. 8 (A) illustrates SWV results, highlighting that the increase in peak intensity of CPE-TPM confirms the increase in the amount of polymer formed on the electrode, as a function of monomer concentration. As monomer concentration increased, so did the amount of polymer, leading to an increase in both cathodic and anodic peaks.

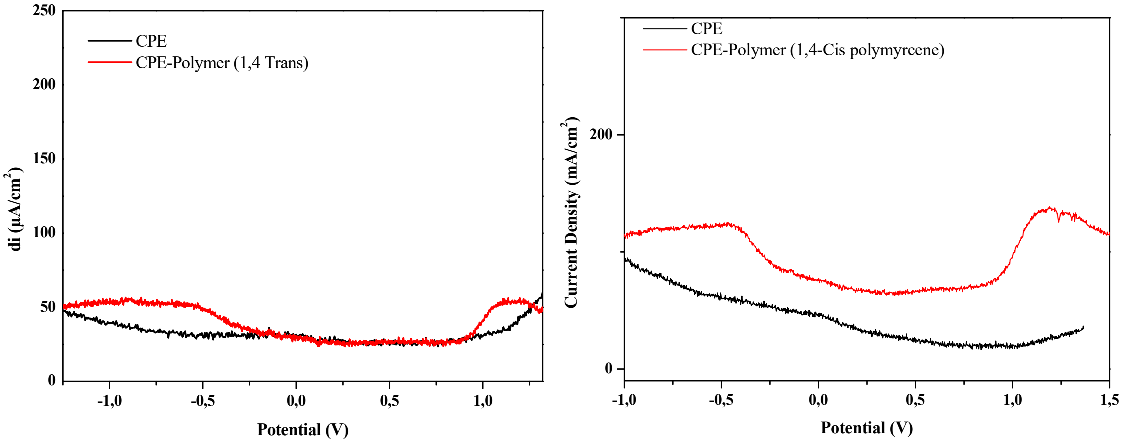

(A) **(B)**

Figure 8: CV recorded by SWV of **(A)**- CPE **(B)**- and CPE/TPM in 1 M NaCl, at SR of 50 mV/s and PH 7.

The shift in the cathodic peak towards more negative values suggests that CPM reduction becomes more difficult with increasing monomer concentration. This increased difficulty may be due to enhanced interaction between polymer chains, which hinders the reduction of individual monomers.

The stability of the anodic peak potential indicates that CPM oxidation process was not altered by monomer concentration. The nature of CPM oxidation appeared to remain constant, irrespective of the polymer amount present on CPE. Fig. 8 (B) shows CPE modified with CPM, demonstrating an increase in the electrode activity. This improvement was due to the increased active surface area of CPE and the improved electrical conductivity of CPM.

Comparison of two polymers

Difference between two polymers by CV

Fig. 9 shows CV of TPM and CPM. An important observation is that TPM polymer displays a higher potential than CPM, a phenomenon due to differences in chemical structures between them. TPM exhibits a more ordered linear structure, while CPM is characterized by a more disordered branched structure. It is worth noting that peak current of TPM was higher than that of CPM, suggesting greater electrochemical reactivity for the former. In addition, peak potential of TPM is at more positive values than that of CPM, indicating higher oxidation for TPM. The peak of TPM is also narrower, which suggests a more reversible oxidation process that that from CPM.

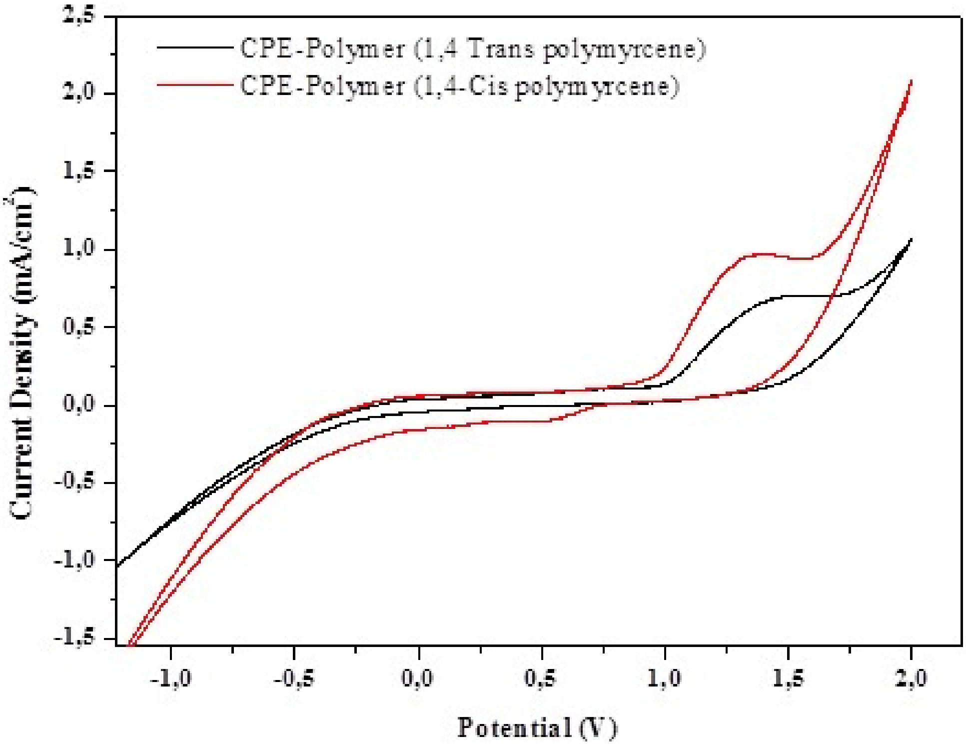

Figure 9: CV of CPE-TPM and CPE-CPM in 1 M NaCl, at SR of 50 mV/s and PH 7.

Significant differences by EIS

Fig. 10 shows EIS of a CPE electrode and a polymer-modified CPE. It can be seen that the diameter of CPE-TPM is larger at high frequencies, indicating slower diffusion of ions.

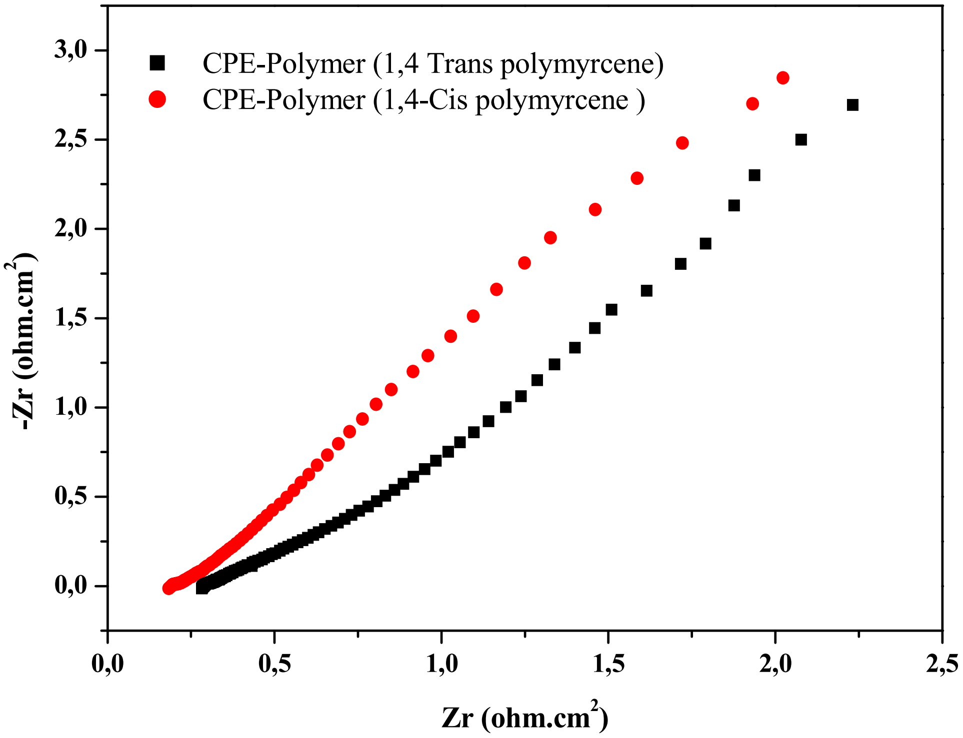

Figure 10: EIS plots of CPE-TPM and CPE- CPM in 1 M NaCl at PH 7.

At low frequencies, the diameter was smaller, which suggests easier electron transfer. In contrast, CPE-CPM diameter is smaller at high frequencies, indicating faster ion diffusion. At low frequencies, the diameter was larger, which indicates more difficult electron transfer. This observation led to the conclusion that TPM had increased resistance to electrical conduction at high frequencies and higher capacity to impede ion passage, compared with CPM. On the other hand, CPM offered greater electrical energy storage capacity than TPM. Consequently, TPM is particularly suitable for applications requiring high resistance to high-frequency electrical conduction, such as capacitors and electrical insulators.

Conclusions

CV can be used to monitor the impact of monomer concentration on the polymerization of TPM on an electrode, enabling the determination of certain polymerization parameters. This information is invaluable for developing new polymer materials and optimizing polymerization processes. Similarly, SWV curve offers the possibility of monitoring the influence of monomer concentration on TPM polymerization on CPE, and determining its parameters. These data are crucial for developing new polymer materials and improving polymerization processes.

Distinctions between CV of TM and CPM have significant implications for their potential applications. TPM is more suitable for applications requiring high electrochemical reactivity, such as batteries and supercapacitors. In contrast, CPM is more suitable for applications where high electrochemical stability is essential, such as sensors and electrodes.

Comparative analysis of EIS diagrams revealed significant differences between TPM and CPM. The choice of the optimum polymer will depend on the final application and electrochemical properties required.

Authors' contributions

S. Loughmari and **M. Oubaouz**: conceptualization, experimental investigation, data analysis, and writing of the original version, as well as subsequent revisions and editing. **M. Oukbab, H. Haddouchy** and **S.-E El Qouatli**: conceptualization. **A. El Bouadili** and **M. Visseaux**: data analysis. **A. Chtaini**: contributed to data analysis and methodology; provided supervision.

Abbreviations

$Al(i\text{-}Bu)_3$: Triisobutyl aluminum
$B(C_6F_5)_3$: Tris(pentafluorophenyl)borane
BEM: n-butylethylmagnesium
C_7H_8: Toluene
$C_{10}H_{16}$: Myrcene
CPE: Carbon paste electrode
CPM: 1,4-cis polymyrcene
CV: Cyclic voltammetry
EIS: Electrochemical impedance spectroscopy
MNZ: Metronidazole
NaCl: Sodium chloride
$Nd(BH_4)_3(THF)_3$: Neodymium trisborohydride
NMR: Nuclear magnetic resonance
PM: Polymyrcene
SWV: Square-wave voltammetry
THF: Tetrahydrofuran
TPM: 1,4-transpolymyrcene

References

1. Tadjik S, Beitollahi H, Néjad FG et al. Recent developments in conductive polymers: applications for electrochemistry. RSC Adv. 2020;10(62):37834-37856. https://doi.org/10.1039/D0RA06160C

2. Teràn-Alcocer À, Bravo-Plascencia F, Cevallos-Morillo C et al. Electrochemical sensors based on conductive polymers for aqueous detection of biologically relevant molecules. Nanomaterials. 2021;11(1):252. https://doi.org/10.3390/nano11010252
3. Palma-Cando A, Woitassek D, Brunklaus G et al. Luminescent tetraphenylethene-cored, carbazole- and thiophene-based microporous polymer films for the chemosensing of nitroaromatic analytes. Mater Chem. Front. 2017;1:1118-1124. https://doi.org/10.1039/C6QM00281A
4. Samal K, Mahapatra S, Hibzur AM. Pharmaceutical wastewater as Emerging Contaminants (EC): Treatment technologies, impact on environment and human health. Ener Nexus. 2022;6(16):100076. https://doi.org/10.1016/j.nexus.2022.100076
5. Aarab N, Hsini A, Essekri A et al. Removal of an emerging pharmaceutical pollutant (metronidazole) using PPY-PANi copolymer: Kinetics, equilibrium and DFT identification of adsorption mechanism. Groundwat Sustain Devel. 2020;11:100416. https://doi.org/10.1016/j.gsd.2020.100416
6. Salimi A, Izadi M, Hallaj R et al. Simultaneous Determination of Ranitidine and Metronidazole at Glassy Carbon Electrode Modified with Single Wall Carbon Nanotubes. Electroanalysis. 2007;19(16):1668-1676. https://doi.org/10.1002/elan.200703911
7. Sotzing GA, Reddinger JL, Katritzky AR et al. Multiply Colored Electrochromic Carbazole-Based Polymers. Chem Mater. 1997;9(7):1578-1587. https://doi.org/10.1021/CM960630T
8. Goldblatt LA, Samuel P. Process for converting nopinene to myrcene. US2420131. U.S. Patent, 1947.
9. Behr A, Johnen L. Myrcene as a natural base chemical in sustainable chemistry: a critical review. Chem Sus Chem. 2009;2(12):1072-1095. https://doi.org/10.1002/cssc.200900186C
10. Wang W, Lu W, Goodwin A et al. Recent advances in thermoplastic elastomers from living polymerizations: Macromolecular architectures and supramolecular chemistry. Progr Polym Sci. 2019;95:1-31. https://doi.org/10.1016/j.progpolymsci.2019.04.002
11. Hilschmann J, Kali G. Bio-based polymyrcene with highly ordered structure via solvent free controlled radical polymerization. Europ Polym J. 2015;73-363-373. https://doi.org/10.1016/j.eurpolymj.2015.10.021
12. Jia X, Li W, Zhao J et al. Dual Catalysis of the Selective Polymerization of Biosourced Myrcene and Methyl Methacrylate Promoted by Salicylaldiminato Cobalt(II) Complexes with a Pendant Donor. Organometallics. 2019;38(2):278-288. https://doi.org/10.1021/acs.organomet.8b00708

13. Loughmari S, Hafid A, Bouazza A et al. Highly stereoselective coordination polymerization of β-myrcene from a lanthanide-based catalyst: Access to bio-sourced elastomers. J Polym Sci A Polym Chem. 2012;50(14):2898-2905. https://doi.org/10.1002/pola.26069
14. Georges S, Bria M, Zinck P et al. Polymyrcene microstructure revisited from precise high-field nuclear magnetic resonance analysis. Polymer. 2014;55(16):3869-78. https://doi.org/10.1016/j.polymer.2014.06.021
15. Loughmari S, Visseaux M, Bouazza A et al. Synthesis of myrcene - isoprene copolymer. Arkivoc. 2023;8:202312045. https://doi.org/10.24820/ark.5550190.p012.045
16. Loughmari S, Visseaux M, El Bouadili A. Valorization of bioresources for the production of polymer using lanthanide borohydride as catalysts. Stud UBB Chem. 2024;69(1);187-200. https://doi.org/10.24193/subbchem.2024.1.12
17. Lamparelli D H, Paradiso V, Monica FD et al. Toward More Sustainable Elastomers: Stereoselective Copolymerization of Linear Terpenes with Butadiene. Macromolecules. 2020;53(5):1665-1673. https://doi.org/10.1021/acs.macromol.9b02646
18. Hulnik MI, Vasilenko IV, Radchenko AV et al. Aqueous cationic homo-and co-polymerizations of β-myrcene and styrene: a green route toward terpene-based rubbery polymers. Polym Chem. 2018;9(48):5690-5700. https://doi.org/10.1039/C8PY01378K
19. Métafiot A, Kanawati Y, Gérard JF et al. Synthesis of β-Myrcene-Based Polymers and Styrene Block and Statistical Copolymers by SG1 Nitroxide-Mediated Controlled Radical Polymerization. Macromolecules. 2017;50(8):3101-3120. https://doi.org/10.1021/acs.macromol.6b02675
20. Daniel J, Pichot C. Synthetic latexes. Development, properties, applications. Editions Lavoisie. 2006.
21. Save M, Hellaye ML, De Villedon V et al. Biosourced Polymeric Emulsifiers for Miniemulsion Copolymerization of Myrcene and Styrene: Toward Biobased Waterborne Latex as Pickering Emulsion Stabilizer. Biomacromolecules. 2022;23(6):2536-2551. https://doi.org/10.1021/acs.biomac.2c00257
22. Mirsaidov U, Shaimuradov IB, Khikmatov M. X-Ray Diffraction Study of Tristetrahydrofuranates of Tetrahydroborates of Lanthanum, Neodymium and Lutetium. Zhur Neorgan Khim. 1986;31(5):1321-1323.